RSC Advances

PAPER

Cite this: *RSC Adv.*, 2016, **6**, 107416

A non-covalent interaction of Schiff base copper alanine complex with green synthesized reduced graphene oxide for highly selective electrochemical detection of nitrite

Subramanian Sakthinathan,[a] Subbiramaniyan Kubendhiran,[a] Shen-Ming Chen,*[ac] Fahad M. A. Al-Hemaid,[c] Wei Cheng Liao,[a] P. Tamizhdurai,[b] S. Sivasanker,*[b] M. Ajmal Ali[c] and A. A. Hatamleh[c]

Received 15th August 2016
Accepted 15th October 2016

DOI: 10.1039/c6ra20580a

www.rsc.org/advances

A novel and selective nitrite sensor based on non-covalent interaction of Schiff base copper complex [Cu(sal-ala)(phen)] with reduced graphene oxide (RGO) was developed by simple eco-friendly approach. The morphology of the prepared RGO/[Cu(sal-ala)(phen)] nanocomposite was characterized by scanning electron microscopy (SEM), ultraviolet visible spectroscopy (UV), electrochemical impedance spectroscopy (EIS), energy dispersive X-ray spectroscopy, X-ray diffraction studies and Fourier transform infrared spectroscopy (FT-IR). On the other hand, the electrochemical studies of the prepared nanocomposite was investigated by cyclic voltammetry (CV) and amperometric technique. The RGO/[Cu(sal-ala)(phen)] nanocomposite modified glassy carbon electrode (GCE) exhibit the higher electrocatalytic activity towards detection of nitrite. Moreover, the RGO/[Cu(sal-ala)(phen)] modified GCE was determined the nitrite with low detection limit (19 nM), broad linear range (0.05–1000 μM) and high sensitivity (3.86 μA μM^{-1} cm^{-2}). Besides, the proposed sensor shows good selectivity, repeatability, reproducibility and long term operational stability. The appreciable recoveries was achieved for the detection of nitrite in water and sausage samples, which imply the practical feasibility of the modified electrode.

1. Introduction

Nitrites are inorganic compounds and are widely used in food additives, corrosion inhibitors and fertilizing agents.[1,2] They can easily contaminate drinking water due to human activities, industrial pollutants and fertilizing agents.[3] The maximum permissible level of nitrite in drinking water is 1 mg L^{-1} and excess of nitrite can causes several health problems like blue baby syndrome and shortness of breath. Moreover, nitrite can readily react with hemoglobin to form methemoglobin, which causes oxygen deficiency in blood.[4,5] Besides, nitrite can react with various amines to form *N*-nitrosamines which cause stomach cancer to humans. Therefore, the determination of nitrite in food, drinking water and environmental samples is very important.[6] To date, several analytical methods have been developed for the detection of nitrite, including chromatographic methods,[7] capillary electrophoresis,[8] chemiluminescence,[9] ion exchange chromatographic[10] and electrochemical methods.[11] Compared with other traditional analytical methods, electrochemical methods are widely used for the detection of nitrite due to high sensitivity, simplicity and selectivity.[12,13] Unmodified electrodes are active towards detection of nitrite. However, the working potential was higher and selectivity also poor in the presence of interfering compounds. Hence, chemically modified electrodes were used for the detection of nitrite due to lowest oxidation potential and higher sensitivity.

Graphene is a two dimensional hexagonal carbon lattice with sp^2 hybridization. It has widespread application because of its unique physicochemical properties such as high surface area, chemical stability, high electrical conductivity and extraordinary mechanical properties.[14,15] Comparatively, reduced graphene oxide (RGO) has superior conductivity compared to GO due to the more active edge plane defects and large effective surface area,[16] so we need to find suitable methods for reducing GO. Nowadays, different kinds of methods have been used for the preparation of RGO, which includes chemical vapor deposition (CVD),[17] mechanical

[a]*Electroanalysis and Bioelectrochemistry Lab, Department of Chemical Engineering and Biotechnology, National Taipei University of Technology, No. 1, Section 3, Chung-Hsiao East Road, Taipei 106, Taiwan, Republic of China. E-mail: smchen78@ms15.hinet.net; Fax: +886 2270 25238; Tel: +886 2270 17147*

[b]*National Centre for Catalysis Research, Indian Institute of Technology, Chennai-600036, India. E-mail: ssivasanker@iitm.ac.in*

[c]*Department of Botany and Microbiology, College of Science, King Saud University, Riyadh 11451, Saudi Arabia*

exfoliation,[18] electric arc discharge,[19] thermal reduction[20] and chemical reduction.[21] Among all methods, chemical reduction is a more suitable and versatile method for the preparation of RGO in bulk quantities. However, in this method toxic and explosive chemicals are used for RGO preparation. Therefore, we need to explore environmentally friendly reducing agents for the effective reduction of GO.[22] Incidentally, caffeic acid provides a good platform for the reduction of GO, because caffeic acid (CA) is one of the hydroxyl cinnamic acids and it has good antioxidant properties. Moreover, the structure of CA has two adjacent hydroxyl groups an aromatic ring, which helps donation of hydrogen to the GO reduction. Therefore, CA is considered a green, effective and low cost reducing agent for RGO preparation.[23]

Schiff base complexes have an azomethine group (–HC═N–) that plays an important role in co-ordination chemistry. The Schiff bases are used to form stable complexes with transition metal ions. In addition, the Schiff base complexes are functionalized with RGO and used for different kinds of applications like sensors, catalysis and energy storage applications.[24–26] Besides, the non-covalent functionalization has advantages over covalent functionalization, because it avoids destruction and retains the unique properties of graphene. [27,28] In this work we have synthesized the RGO/[Cu(sal-ala)phen] (sal-ala = salicylalanine-alanine, phen = 1,10-phenanthroline) nanocomposite by non-covalent interaction. To the best of our knowledge this is the first time a Schiff base copper complex [Cu(sal-ala)phen] undergoes noncovalent interaction with RGO to prepare a new type of nanocomposite for the electrochemical detection of nitrite.

2. Experimental

2.1 Reagent and solution

Graphite powder (size < 20 μm), sodium nitrite, caffeic acid, L-alanine were purchased from Sigma Aldrich. 1,10-Phenanthroline, copper(II) chloride monohydrate and salicylaldehyde were purchased from Merck chemical. The phosphate (0.05 M) buffer solution (PBS) was prepared by using Na_2HPO_4 and NaH_2PO_4, the pH was adjusted by H_2SO_4 or NaOH. All the chemicals used in this work were of analytical grade and used without any further purification. Prior to each experiment, the electrolyte solutions were deoxygenated with purified N_2 for 15 min. All the experiments were carried out at room temperature and all the required solutions were made up using double distilled water.

2.2 Experimental apparatus

Electrochemical studies were carried out at the CHI 410 electrochemical work station. The electrochemical cell contains GCE as a working electrode, Ag/AgCl as a reference electrode and Pt wire as a counter electrode. The electrochemical experiments were performed in N_2 saturated electrolyte. UV-visible spectra were taken on a Perkin Elmer spectrophotometer and electrochemical impedance spectra were carried out on EIM6EX ZAHNER equipment, Kroanch, Germany. Scanning electron (SEM) microscope studies were carried out using a Hitachi S-3000H microscope. Elemental analysis was carried out using HORIBA EMAX X-ACT (model 51-ADD0009). Powder X-ray diffraction (XRD) studies were performed XPERT-PRO (Netherlands) diffractometer using Cu Kα radiation (k = 1.54 Å). Fourier transform infrared spectroscopy (FT-IR) was carried out using a Jasco FT-IR 6600 spectrometer.

2.3 Preparation of [Cu(sal-ala)(phen)] complex

The inorganic complex was synthesized based on previous reports with slight modifications.[29–32] 1,10-Phenanthroline (5 mmol; 0.99 g in 20 mL methanol) and salicylalanine (5 mmol; 0.97 g in 20 mL methanol) ligands were mixed and homogenized. Then the homogenized solution was added dropwise to a solution of $CuCl_2 \cdot H_2O$ (5 mmol; 0.86 g in 20 mL water) while stirring at 50 °C. A bright green precipitate of [Cu(sal-ala)(phen)] complex was obtained (Scheme 1), and this precipitate was filtered and washed with ethanol then dried in a desiccator. The prepared Schiff base complex was confirmed by the UV visible and FT-IR spectroscopy.

2.4 Preparation of RGO/[Cu(sal-ala)(phen)] inorganic nanocomposite

Graphene oxide was prepared from graphite by modified Hummers method.[33] The RGO was prepared by the following procedure of Bo *et al.*[34] 10 mg of GO was dispersed in 100 mL deionized water and caffeic acid (CA) (5 mg) was added to the GO dispersion. The mixture was then heated at 95 °C for 24 hours in an oil bath with the assistance of stirring. The resulting suspension was collected and washed with deionized water and ethanol. Finally, the prepared RGO was dried at 35 °C under vacuum conditions.

The non-covalent approach was used to prepare the RGO/[Cu(sal-ala)(phen)] nanocomposite with distinctive electrocatalytic activity towards the oxidation of nitrite.[35] The nanocomposite was synthesized by dispersing the RGO in DMF and further addition of [Cu(sal-ala)(phen)] under vigorous stirring. Then, the obtained homogeneous solution was subjected to ultrasonic treatment (30 min) for enhancing the interaction between RGO and [Cu(sal-ala)(phen)]. The resultant homogeneous RGO/[Cu(sal-ala)(phen)] nanocomposite was filtered and washed with ethanol three times and dried in oven. Finally, the prepared RGO/[Cu(sal-ala)(phen)] was re-dispersed in DMF (1 mL) and drop casted on the cleaned GCE surface then dried in room temperature. Scheme 2 displays the preparation of GCE/RGO/[Cu(sal-ala)(phen)] modified electrode for the electrochemical detection of nitrite.

3. Result and discussion

3.1 Characterization of prepared nanocomposite

Fig. 1 shows the SEM images of (A) GO, (B) RGO, (C) GO/[Cu(sal-ala)(phen)], (C′) [Cu(sal-ala)(phen)], (D) RGO/[Cu(sal-ala)(phen)]. The SEM image of graphene oxide shows a thin and wrinkled surface. In addition, RGO exhibited randomly

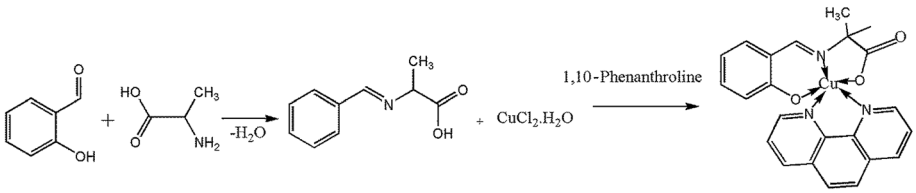

Scheme 1 Synthesis of [Cu(sal-ala)(phen)] inorganic complex.

aggregated with distinct edges and folding sheet surfaces. The SEM image of GO/[Cu(sal-ala)(phen)] exhibit the Schiff base copper complex incorporated on the GO surface and the inset Fig. 1C′ shows the SEM image of [Cu(sal-ala)(phen)] complex. From the SEM image of RGO/[Cu(sal-ala)(phen)] nanocomposite it can be observed that the [Cu(sal-ala)(phen)] inorganic complex was uniformly covered on the RGO surface. Furthermore, the elemental composition of as-prepared nanocomposite was explored by elemental analysis. Fig. 1E and F displayed the EDX spectra of RGO/[Cu(sal-ala)(phen)] nanocomposite, where the signals for carbon, oxygen, nitrogen and copper confirmed the formation of nanocomposite. Notably, the signals of copper and nitrogen confirm the Schiff base formation and complexation.

Electrochemical impedance spectroscopy (EIS) has been used to understand the charge transfer resistance (R_{ct}) of the different modified electrodes at the electrode and electrolyte interface. Fig. 2A shows the EIS plots of (a) bare GCE, (b) GCE/RGO, (c) GCE/[Cu(sal-ala)(phen)], (d) GCE/GO/[Cu(sal-ala)(phen)], (e) GCE/RGO/[Cu(sal-ala)(phen)] in 5 mM $[Fe(CN)_6]^{3-/4-}$ with 0.1 M KCl as a supporting electrolyte. The diameter of the semicircle corresponds to the charge transfer resistance (R_{ct}) of the modified electrodes. A higher R_{ct} value of about 1561 Ω was observed for the GCE/[Cu(sal-ala)(phen)] modified electrode. The bare GCE and GCE/RGO show R_{ct} values of 378 Ω and 244 Ω, respectively. However, the R_{ct} value of the GCE/GO/[Cu(sal-ala)(phen)] modified electrode was about 235 Ω, which indicates that the charge transfer resistance of Schiff base copper complex was decreased due to the non-covalent interaction with GO. Interestingly, the GCE/RGO/[Cu(sal-ala)(phen)] modified electrode shows a low R_{ct} value of 33 Ω due to the reduction of GO to RGO, which enhance the conductivity of the modified electrode. The EIS results confirmed that the GCE/RGO/[Cu(sal-ala)(phen)] modified electrode have higher electron transfer properties with low charge transfer resistance. The UV-visible spectra were used to identify the structural information about the nanocomposites. Fig. 2B shows the UV visible spectra of (a) RGO, (b) [Cu(sal-ala)(phen)] and (c) RGO/[Cu(sal-ala)(phen)]. The synthesized RGO shows an absorbance peak at 283 nm; it confirms that the GO was successfully reduced by CA with the eco-friendly route. Furthermore, there is an absorbance peak at 222 nm for the π–π* transition of phenanthroline and 272 nm for n–π* transition of the salicylidene. The Cu(II) complex shows a peak at 372 nm due to the ligand to metal charge transfer transition and RGO/[Cu(sal-ala)(phen)] shows the peaks that were observed in the free base which confirms the formation of nanocomposite.[36]

Fig. 3A shows the X-ray diffraction studies of (a) RGO, (b) [Cu(sal-ala)(phen)], (c) RGO/[Cu(sal-ala)(phen)]. The XRD pattern of RGO shows a broad peak at 26° due to the short range order for stacked layer. On the other hand, the XRD spectra of [Cu(sal-ala)(phen)] show peaks at 11°, 12.6°, 17°, 19°, 22° and 25°, which confirms the formation of a Schiff base copper(II) complex. Besides, the peaks in the XRD spectra of RGO/[Cu(sal-ala)(phen)] observed at 11°, 12°, 25°, 30°, 41° and 69° are quite similar to those of [Cu(sal-ala)(phen)].[37] However, the intensity has decreased and the peak shapes are

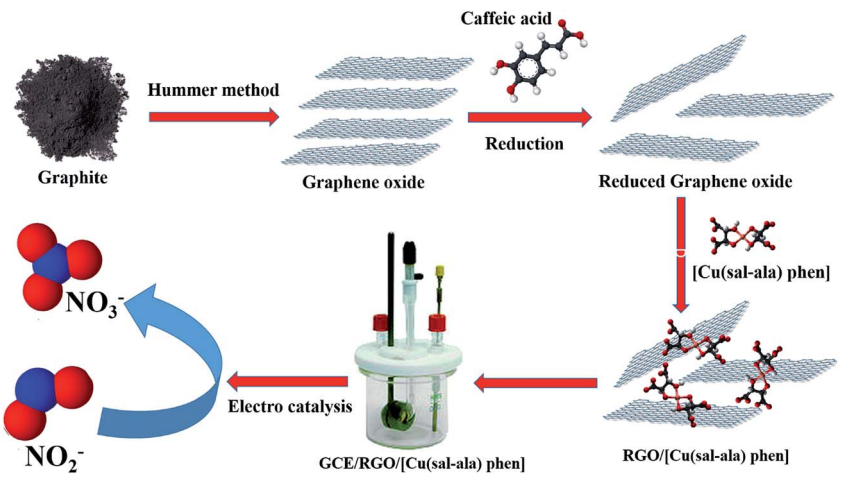

Scheme 2 Schematic representation for the preparation of RGO/[Cu(sal-ala)(phen)] nanocomposite for nitrite sensor.

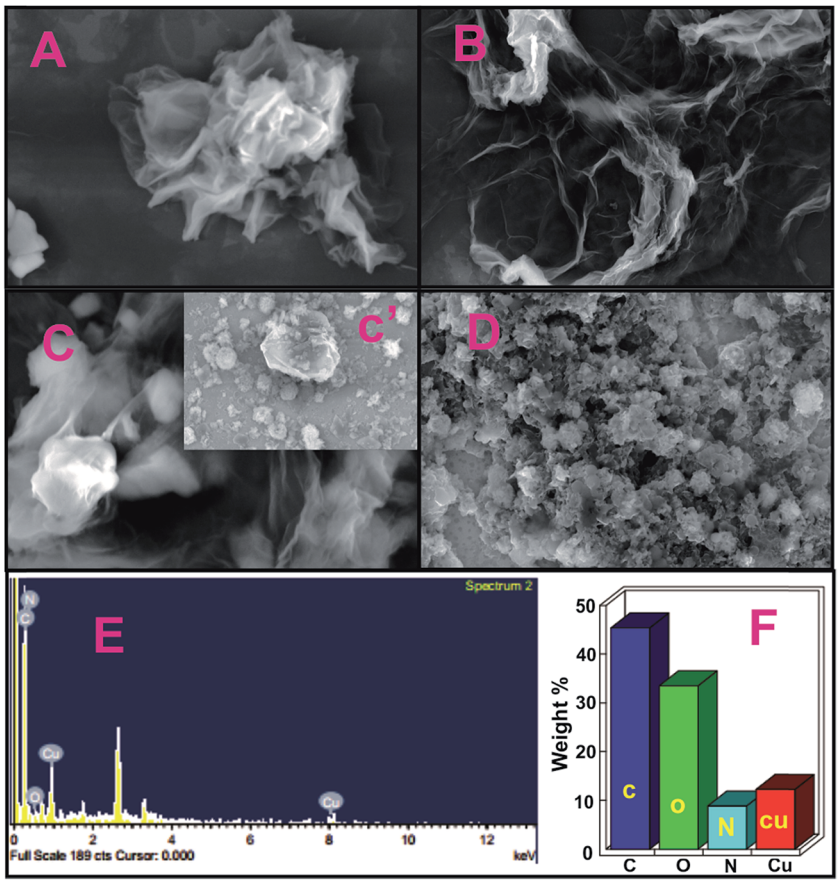

Fig. 1 SEM images of (A) GO, (B) RGO, (C) GO/[Cu(sal-ala)(phen)], (D) RGO/[Cu(sal-ala)(phen)], (inset C') [Cu(sal-ala)(phen)], (E & F) EDX spectrum of RGO/[Cu(sal-ala)(phen)] nanocomposite.

different. These results confirmed the formation of RGO/[Cu(sal-ala)(phen)] nanocomposite. The surface chemistry, bonding nature and chemical structure of the prepared nanocomposite were characterized by FT-IR spectra. Fig. 3B shows the FT-IR spectra of (a) RGO, (b) [Cu(sal-ala)(phen)], (c) RGO/[Cu(sal-ala)(phen)]. The FT-IR spectrum of RGO exhibited the characteristic peak at 3452 cm^{-1} for the stretching vibration of hydroxyl groups. Moreover, the peaks observed at 1725 cm^{-1} and 1229 cm^{-1} correspond to the stretching vibrations of C=O and C–O. The stretching vibration peak appeared at 833 cm^{-1} for the C–H rocking vibration which confirms the phenanthroline functionalities in [Cu(sal-ala)(phen)]. The peak in the region of 2063 cm^{-1} indicate N–H bonds of the Schiff base complex. The Cu–O band appeared at 930 cm^{-1} and Cu–N appeared at 528–549 cm^{-1}. The peask at around 2918 cm^{-1} and 2892 cm^{-1} can be assigned to C–H and CH_2 stretching vibration, respectively. The FT-IR spectrum of RGO/[Cu(sal-ala)(phen)] nanocomposite shows stretching vibrations similar to RGO and [Cu(sal-ala)(phen)].[33] The FT-IR results confirmed that the Schiff base copper complex interacts non-covalently with RGO and leads to formation of composite.

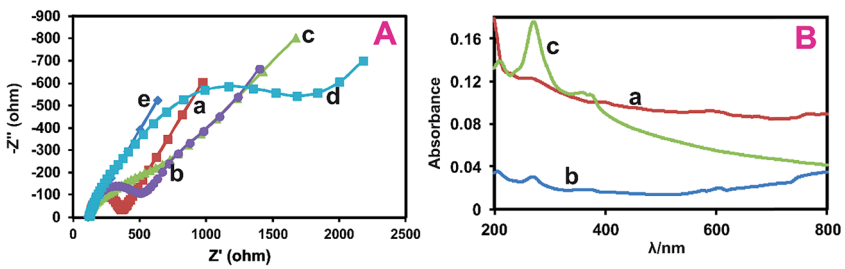

Fig. 2 (A) Electrochemical impedance spectra of (a) bare GCE (b) GCE/RGO, (c) [Cu(sal-ala)(phen)], (d) GO/[Cu(sal-ala)(phen)] and (e) RGO/[Cu(sal-ala)(phen)] modified electrode in 0.1 M KCl containing 5 mM $[Fe(CN)_6]^{3-/4-}$. (B) UV-Vis spectroscopic analysis of (a) RGO, (b) [Cu(sal-ala)(phen)] and (c) RGO/[Cu(sal-ala)(phen)].

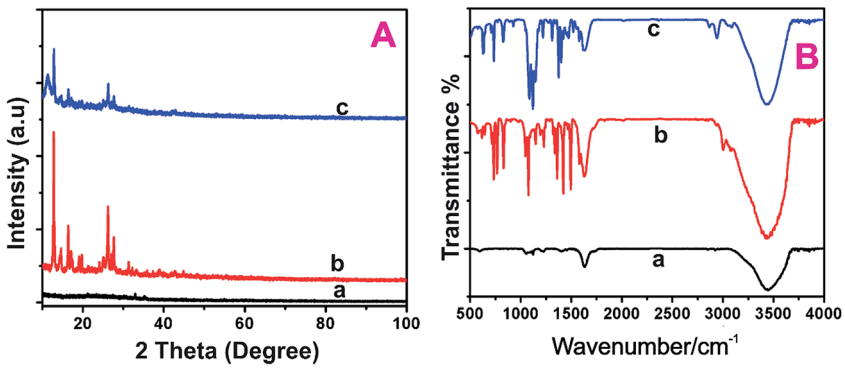

Fig. 3 (A) X-ray diffraction studies of (a) RGO, (b) [Cu(sal-ala)(phen)], (c) RGO/[Cu(sal-ala)(phen)]. (B) FT-IR spectra of (a) RGO, (b) [Cu(sal-ala)(phen)], (c) RGO/[Cu(sal-ala)(phen)].

4. Electrocatalytic oxidation of nitrite

4.1 Electrocatalytic oxidation of nitrite at various modified electrodes and effect of different concentration

Fig. 4A shows the CV curves of (a) RGO/[Cu(sal-ala)(phen)] nanocomposite modified electrode in the absence of nitrite and (b) bare GCE, (c) GO, (d) [Cu(sal-ala)(phen)], (e) RGO, (f) GO/[Cu(sal-ala)(phen)], (g) RGO/[Cu(sal-ala)(phen)] nanocomposite modified electrodes in the presence of 200 μM nitrite in PBS (pH 5). The bare GCE and GO modified electrodes oxidize nitrite at the peak potential (E_P) of 0.99 V and 0.98 V with corresponding oxidization peak currents of (I_P) 25.23 μA and 27.38 μA, respectively. In addition, the [Cu(sal-ala)(phen)] modified electrode displays E_P and I_P of about 1.056 V and 30.64 μA. Besides, the RGO modified electrode exhibits E_P of 0.964 V and I_P of 31.33 μA for the oxidation of nitrite. Furthermore, the GO/[Cu(sal-ala)(phen)] modified electrode shows E_P and I_P at 0.93 V and 43.9 μA, respectively, for the oxidation of nitrite. Comparatively the oxidation peak current of nitrite was increased for the GO/[Cu(sal-ala)(phen)] modified electrode compared to [Cu(sal-ala)(phen)] and RGO modified electrodes. These results confirmed the formation of non-covalent interaction between the GO and [Cu(sal-ala)(phen)], which enhanced the catalytic activity. Generally, RGO shows better electrocatalytic properties than GO because the GO contains many oxygen functionalities, which create internal resistance at the modified electrode. In this aspect, the RGO/[Cu(sal-ala)(phen)] nanocomposite was prepared and applied for the determination of nitrite as an alternative to GO/[Cu(sal-ala)(phen)]. As expected, the RGO/[Cu(sal-ala)(phen)] nano composite exhibits a substantial oxidization peak potential at (E_P) 0.97 with an improved oxidation peak current (I_P) of 49.80 μA, which are comparatively higher than that of all aforementioned modified electrodes. These results can be attributed to the non-covalent interaction of RGO and [Cu(sal-ala)(phen)], which plays an important role in the oxidation of nitrite due to their extraordinary electrocatalytic activity. Hence, the RGO/[Cu(sal-ala)(phen)] nanocomposite modified electrode proved to be excellent for use as a nitrite sensor. Fig. 4B shows the CV curves of RGO/[Cu(sal-ala)(phen)] nanocomposite modified electrode for the oxidation of nitrite in various concentrations of nitrite containing PBS (pH 5) at a scan rate of 50 mV s^{-1}. Increasing the concentration of nitrite from 50 μM to 600 μM, resulted in the oxidized peak current to increase linearly. The Fig. 4B inset shows the linear relationship between the peak current *vs.* concentration, and the corresponding linear regression equation can be expressed as $I_{pa} = 0.5074x - 40.813$ with a correlation coefficient $R^2 = 0.9947$. It is evident that the RGO/[Cu(sal-ala)(phen)] nanocomposite modified GCE electrode has good electrocatalytic activity towards the detection of nitrite.

4.2 Effect of pH and scan rate

The influence of pH on the performance of an as-prepared modified electrode for the detection of nitrite was investigated using CV. The CV experiment was recorded at RGO/[Cu(sal-ala)(phen)] modified GCE at various pHs ranging from 1 to 9 towards the electrocatalytic oxidation of 200 μM nitrite. As shown in the Fig. 5A, the oxidation peak current of nitrite increased when increasing the electrolyte pH from 1 to 5, and afterwards it decreases by varying the pH from 6 to 9. This result showed that, at lower pH the NO_2^- ions are unstable so they can be easily converted to NO and NO_3^-. At the same time at higher pHs, a proton deficiency occurred. However, at pH 5 the sensor exhibited higher electrocatalytic performance (Fig. 5B). Therefore, we chose pH 5 for further electrochemical studies. Fig. 6A shows a typical CV curve obtained at the RGO/[Cu(sal-ala)(phen)] modified electrode for the different scan rates in PBS (pH 5) containing 200 μM nitrite. The results showed that the peak current linearly increased with respect to the increasing scan rates from 0.01 to 0.11 V s^{-1}. Fig. 6B shows a corresponding plot of peak current (I_P) *vs.* square root of scan rate ($\nu^{1/2}$) and from this the corresponding linear regression equation was calculated as $I_P = 75.58\nu^{1/2}$ (V s^{-1})$^{1/2}$ + 10.60 with $R^2 = 0.998$. From this result, we have concluded that the oxidation of nitrite is a diffusion-controlled process at RGO/[Cu(sal-ala)(phen)].[38] Moreover, the electrocatalytic oxidation of nitrite at a RGO/[Cu(sal-ala)(phen)] modified electrode is an irreversible process and the anodic peak shifted to positive potential when increasing the scan rate. The electron transfer co-efficient and the number of electrons transfer involved in the rate-determining step can be estimated by the following equations

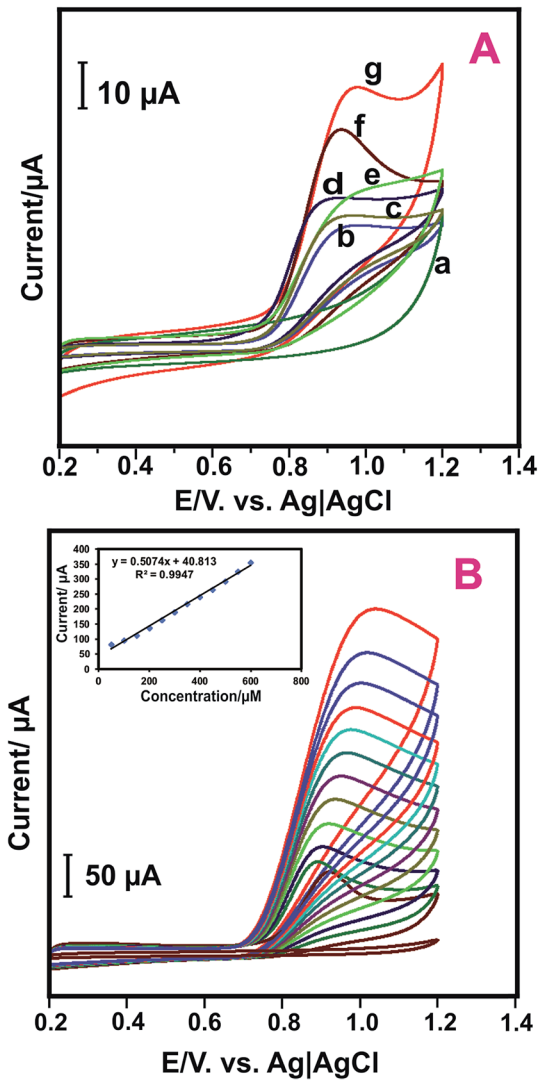

Fig. 4 (A) Cyclic voltammetry of (a) RGO/[Cu(sal-ala)(phen)] nanocomposite modified electrode in absence of nitrite, (b) bare GCE, (c) GCE/GO, (d) GCE/[Cu(sal-ala)(phen)], (e) GCE/RGO, (f) GO/[Cu(sal-ala)(phen)] and (g) RGO/[Cu(sal-ala)(phen)] in 0.05 M PBS (pH 5) containing 200 μM nitrite at scan rate 50 mV s^{-1}. (B) Cyclic voltammetry response of RGO/[Cu(sal-ala)(phen)] nanocomposite at different concentration of nitrite in 0.05 M PBS (pH 5) at scan rate 50 mV s^{-1}.

$$E_{pa} = [2.303RT/2(1 - \alpha)n_aF]\log \nu + K \quad (a)$$

$$I_P = (2.99 \times 10^5)_n[(1 - \alpha)n_a]^{1/2}AC_0 \times D_0{}^{1/2}\nu^{1/2} \quad (b)$$

where K is a constant, n_a is 1 and substituting the slope of E_{pa} *versus* log ν plot in the eqn (a) the value of α was obtained as 0.52 for the nitrite oxidation. Furthermore, the number of electrons involved in the oxidation of nitrite can be estimated by the eqn (b) for a totally irreversible process controlled by diffusion. For eqn (b), D_0 is the diffusion coefficient of nitrite, A is the electrode area and C_0 is the concentration of nitrite. By substituting all the values in the above eqn (b), the value of n is estimated to be 2. This result indicated that the nitrite oxidation leads to NO_3^- as a final product and it is good accordance with the literature. The overall nitrite oxidation reaction can be expressed by eqn (c) and (d)

$$NO_2^- - e^- \rightarrow NO_2 \quad (c)$$

$$2NO_2 + H_2O \rightleftharpoons NO_3^- + NO_2^- + 2H^+ \quad (d)$$

From these results, the electrocatalytic oxidation of nitrite at the RGO/[Cu(sal-ala)(phen)] nanocomposite modified electrode as a two-electron transfer reaction.[39]

4.3 Amperometric determination of nitrite

Fig. 7A shows the amperometric response of a RGO/[Cu(sal-ala)(phen)] nanocomposite modified rotating disc electrode (RDE) recorded at a rotation speed of 2000 rpm. The nitrite was successively added in PBS with 50 s intervals for every addition under the convection mode with an applied working potential (E_{app}) of +0.85 V. Herein, a sharp amperometric signal appeared for the determination of nitrite for the addition of 0.05 μM nitrite. Followed by that addition, the concentration of nitrite was increased to 1000 μM. The resultant oxidation peak current linearly increased with increasing the concentration of nitrite (0.05 to 1000 μM). From this result, we have observed two linear concentration ranges such as 0.05–4 μM (low) and 6–1000 μM (high) for the determination of nitrite and the corresponding calibration plot is shown in Fig. 7B and C, respectively. The sensitivity of the fabricated sensor was calculated to be 3.86 μA μM^{-1} cm^{-2} and the lowest detection limit (LOD) calculated to be about 19 nM. The sensitivity of the proposed sensor was compared with some other graphene based nitrite sensor. Notably, the RGO-MWCNT-Pt/Mb fabricated electrode was used as a nitrite sensor with a sensitivity of 0.1651 μA μM^{-1} cm^{-2} and GNPs/MWCNT modified electrode exhibit a sensitivity of about 2.58 μA μM^{-1} cm^{-2}.[40,41] Many nitrite sensor electrodes have been fabricated on graphene derivatives.[42–44] However, the RGO/[Cu(sal-ala)(phen)] nanocomposite modified electrode exhibited a higher sensitivity (3.86 μA μM^{-1} cm^{-2}) than that of previously reported nitrite sensor electrodes. Hence, it is evident that the Schiff base copper(II) complexes could be an effective electrocatalyst for the oxidation of nitrite due to the higher electron transfer rate and good redox properties. In addition, the high surface area of RGO provides a strong interaction between RGO and [Cu(sal-ala)(phen)]. The RGO/[Cu(sal-ala)(phen)] nanocomposite exhibited acceptable selectivity, a wide linear range and low detection limit of nitrite. These observed analytical results are compared with several others nitrite sensor electrodes as shown in Table 1.

4.4 Interference and real sample studies

We have analyzed the selectivity of RGO/[Cu(sal-ala)(phen)] nanocomposite modified electrode towards the detection of nitrite in the presence of common interference ions such as anions, cations and biological samples. The experimental conditions were similar to those in Section 4.3 and the corresponding amperogram is shown in Fig. 8A. The RGO/[Cu(sal-

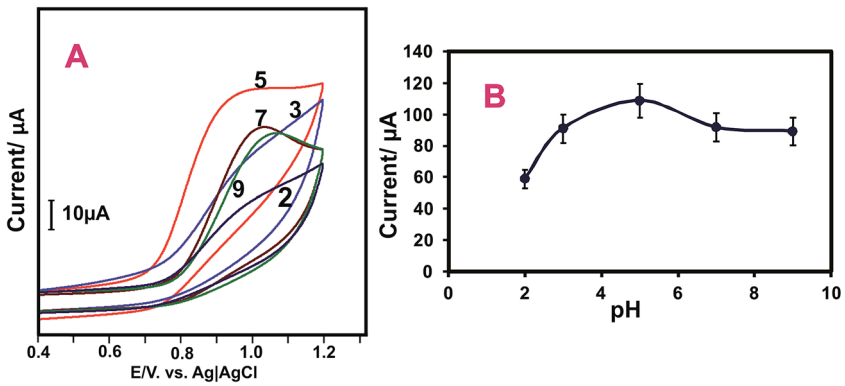

Fig. 5 (A) Cyclic voltammetry response of RGO/[Cu(sal-ala)(phen)] nanocomposite modified GCE in 200 μM nitrite solution at different pH (2, 3, 5, 7, 9 & 11) at a scan rate of 50 mV s^{-1}, (B) calibration plot for pH *vs.* I_P.

ala)(phen)] modified electrode exhibited a good sharp amperometric response for the each 5 μM additions of nitrite (a). Whereas, no response was observed for the 500 μM additions of other interfering ions, such us (b) Br^-, (c) I^-, (d) Cl^-, (e) NO_3^-, (f) F^-, (g) Cu^{2+}, (h) Zn^{2+}, (i) Cr^{2+}, (j) Sr^{2+}, (k) K^+, (l) dopamine, (m) glucose, (n) fructose and (o) ascorbic acid. This study revealed that the RGO/[Cu(sal-ala)(phen)] fabricated electrode selectively detects nitrite even in the presence of excess of other interfering compounds. Therefore, the RGO/[Cu(sal-ala)(phen)] nanocomposite was applied to the detection of nitrite in a real time monitoring application. The practical feasibility of the RGO/[Cu(sal-ala)(phen)] modified sensor has been demonstrated by an amperometric method in water samples of various sources and sausage meat samples. The water samples were collected from a river and lake, the sausage samples were collected from a local market in Taiwan. Before performing the real sample analysis the collected water sample was subjected to filtration to remove the solid suspension. The standard addition method was used for the real sample analysis and the obtained recoveries are 95.6%, 102%, 106% and 103% as shown in Table 2. These results showed that the developed nitrite sensor electrode has acceptable recoveries in real sample analyses. Thus, the modified electrode can be used for the determination of nitrite detection in water and food samples.

4.5 Repeatability, reproducibility and stability studies of RGO/[Cu(sal-ala)(phen)] nanocomposite modified electrode

The repeatability and reproducibility of the proposed sensor was carried out by CV studies in the presence of 200 μM nitrite in PBS (pH 5). The modified electrode exhibited an acceptable repeatability with an RSD of about 3.55% for 10 repetitive measurements examined by a single modified electrode. Moreover, the fabricated sensor electrode shows an appreciable reproducibility of 3.45% for the 10 measurements carried out by 10 different modified electrodes. The obtained results showed that the RGO/[Cu(sal-ala)(phen)] nanocomposite modified electrode has good repeatability and reproducibility. The storage stability of the fabricated electrode was investigated periodically in PBS containing 200 μM nitrite in an inert atmosphere. Fascinatingly, RGO/[Cu(sal-ala)(phen)] exhibited only 3.6% of peak current changes from its initial peak current response after storage for 30 days. The operational stability of the RGO/[Cu(sal-ala)(phen)] nanocomposite modified electrode was carried out by an amperometric technique in the presence of 50 μM nitrite for 3000 s (Fig. 8B). The experimental conditions were similar to those discussed in the Section 4.3 and manifest an oxidized peak current loss of only 2.2% from the initial current. The obtained results reveal the excellent operational stability and antifouling properties of the modified electrode.

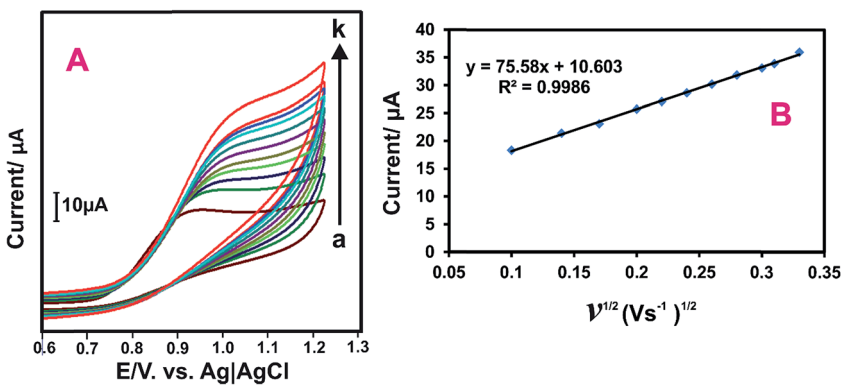

Fig. 6 (A) Cyclic voltammetry response of the RGO/[Cu(sal-ala)(phen)] nanocomposite modified GCE in PBS containing 200 μM of nitrite at different scan rates. (B) Calibration plot of square root of scan rate *vs.* peak current.

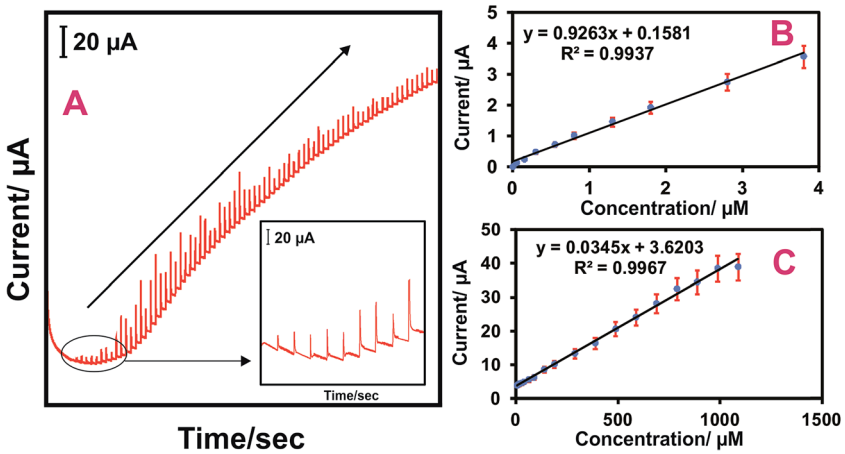

Fig. 7 (A) Amperometric response for the oxidation of nitrite with different concentration in PBS (pH 5), $E_{app} = 0.75$ V. The calibration plot of peak current *vs.* nitrite concentration (low (B) & high (C)).

Table 1 Comparison of the analytical performance of RGO/[Cu(sal-ala)(phen)] nanocomposite modified electrode with other reported sensors

Electrodes	Linear range (μM)	LOD[a] (μM)	References
RGO[b]/[Cu(sal-ala)[c](phen)[d]]	0.05–4, 6–1000	0.019	This work
Poly(methylene blue)/GCE[e]	2.0–5000	2	45
Graphite/β-cyclodextrin	0.7–2150	0.26	46
Thionine modified aligned/CNT[f]	3–5000	1.12	47
RGO–ZnO[g]	10–8000	33	48
Hb[h]/PCAuPs[i]/MWCNT[j]	3.6–3.09	0.96	49
AuNPS[k]/GCE	1–5000	2.4	50
CuO[l]/GCE	5–180	1.6	51
PtNPs[m]	10–1000	5	52
HAC[n]	1–127	70	53
PANI[o] conducting polymer	5–1400	0.24	54
AuNP/graphene/chitosan	1–380	0.25	55

[a] Limit of detection. [b] Reduced graphene oxide. [c] Salicylalanine. [d] Phenanthroline. [e] Glassy carbon electrode. [f] Carbon nanotubes. [g] Zinc oxide. [h] Hemoglobin. [i] Positively charged gold nanoparticle. [j] Multiwalled carbon nanotubes. [k] Gold nanoparticles. [l] Copper oxide. [m] Platinum nano particles. [n] Heteroatom enriched porous carbon. [o] Polyaniline.

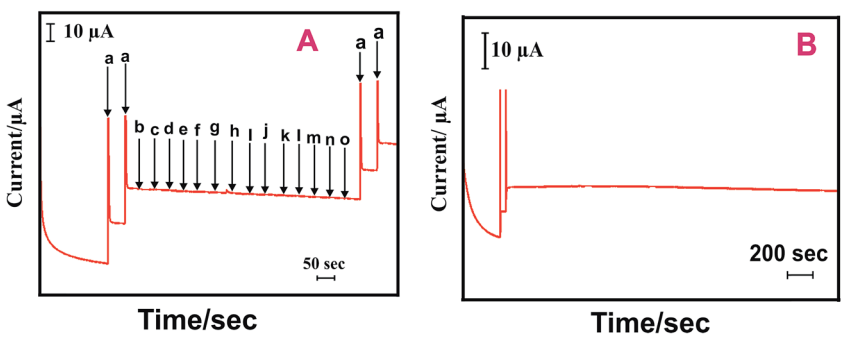

Fig. 8 (A) Amperometric response of hydrazine at RGO/[Cu(sal-ala)(phen)] in the presence of 50 μM nitrite and 500 μM addition of different interferences (b) Br^-, (c) I^-, (d) Cl^-, (e) NO_3^-, (f) F^-, (g) Cu^{2+}, (h) Zn^{2+}, (i) Cr^{2+}, (j) Sr^{2+}, (k) K^+, (l) dopamine, (m) glucose, (n) fructose and (o) ascorbic acid. (B) Stability studies of the RGO/[Cu(sal-ala)(phen)] nanocomposite modified electrode.

Table 2 Determination of nitrite in real samples using RGO/[Cu(sal-ala)(phen)] nanocomposite modified electrode

Samples	Added (μM)	Found (μM)	Recovery (%)	RSD[a] (%)
Tap water	10	9.56	95.6	3.2
River water	10	10.2	102	3.5
Sausage 1	10	10.6	106	3.1
Sausage 2	10	10.3	103	3.2

[a] Relative standard deviation of 3 individual measurements.

5. Conclusions

In summary, we have successfully prepared a novel and stable RGO/[Cu(sal-ala)(phen)] nanocomposite *via* non-covalent interaction and the prepared nanocomposite was characterized by different microscopic and spectroscopic techniques. The RGO/[Cu(sal-ala)(phen)] nanocomposite modified electrode showed excellent electrocatalytic activity towards detection of nitrite with wide linear concentration range (0.05–1000 μM), low detection limit (19 nM) and high sensitivity (3.86 μA μM^{-1} cm^{-2}). The modified electrode offered appreciable repeatability and reproducibility. Moreover, the fabricated electrode selectively determined nitrite ions even in the presence of interfering ions and biological molecules. Moreover, the developed sensor electrode showed good recoveries in real sample analysis of sausage meat and water samples. Therefore, we concluded that the RGO/[Cu(sal-ala)(phen)] nanocomposite modified electrode can be used as an excellent electrode material for the electrochemical detection of nitrite. This proposed sensor electrode can be used in future for the accurate detection of nitrite in food and industrial samples. The reported Schiff base complex has an advantages in terms of ease of preparation, stable complex formation and higher electrochemical activity. Thus, the Schiff base complex based nanomaterials have been extended to develop a new electrochemical sensor.

Acknowledgements

The authors extend their appreciation to the International Scientific Partnership Program ISPP at King Saud University for funding this research work through ISPP#6. Furthermore, this project was supported by the National science council & Ministry of science and technology of Taiwan (ROC).

References

1 S. Palanisamy, B. Thirumalraj and S. M. Chen, *J. Electroanal. Chem.*, 2016, **760**, 97.
2 Y. Haldorai, J. Y. Kim, A. T. E. Vilian, N. S. Heo, Y. S. Huh and Y. K. Han, *Sens. Actuators, B*, 2016, **227**, 92.
3 V. Mani, T. Y. Wu and S. M. Chen, *J. Solid State Electrochem.*, 2014, **18**, 1015.
4 A. Rahim, L. S. S. Santos, S. B. A. Barros, L. T. Kubota, R. Landers and Y. Gushikem, *Electroanalysis*, 2014, **26**, 1.
5 J. P. Salome, R. Amutha, P. Jagannathan, J. J. M. Josiah, S. Berchmans and V. Yegnaraman, *Biosens. Bioelectron.*, 2009, **24**, 3487.
6 L. Cui, J. Zhu, X. Meng, H. Yin, X. Pan and S. Ai, *Sens. Actuators, B*, 2012, **161**, 641.
7 A. Jain, R. M. Smith and K. K. Verma, *J. Chromatogr. A*, 1997, **760**, 319.
8 E. V. Trushina, R. R. Oda, J. P. Landers and C. T. Mcmurray, *Electrophoresis*, 1997, **18**, 1890.
9 F. Yang, M. Troncy, E. Francoeur, B. Vinet, P. Vinay, G. Czaika and G. Blaise, *Clin. Chem.*, 1997, **43**, 657.
10 P. Steinhoff and H. Kelm, *J. Chromatogr. B: Biomed. Sci. Appl.*, 1996, **685**, 348.
11 M. H. Barley, K. J. Takeuchi and T. J. Meyer, *J. Am. Chem. Soc.*, 1986, **108**, 5876.
12 Y. Zhang, Y. Zhao, S. Yuan, H. Wang and C. He, *Sens. Actuators, B*, 2013, **185**, 602.
13 C. Yu, J. Guo and H. Gu, *Electroanalysis*, 2010, **22**, 1005.
14 N. I. Ikhsan, P. Rameshkumar, A. Pandikumar, M. M. Shahid, N. M. Huang, S. V. Kumar and H. N. Lim, *Talanta*, 2015, **144**, 908.
15 G. Bharath, R. Madhu, S. M. Chen, V. Veeramani, D. Mangalaraj and N. Ponpandian, *J. Mater. Chem. A*, 2015, **3**, 15529.
16 S. Sakthinathan, S. Kubendhiran, S. M. Chen, K. Manibalan, M. Govindasamy, P. Tamizhdurai and S. Tung Huang, *Electroanalysis*, 2016, **28**, 1.
17 A. Reina, X. Jia, J. Ho, D. Nezich, H. Son, V. Bulovic, M. S. Dresselhaus and J. Kong, *Nano Lett.*, 2009, **9**, 30.
18 S. Stankovich, D. A. Dikin, R. D. Piner, K. A. Kohlhaas, A. Kleinhammes, Y. Jia, Y. Wu, S. B. T. Nguyen and R. S. Ruoff, *Carbon*, 2007, **45**, 1558.
19 K. S. Subrahmanyam, L. S. Panchakarla, A. Govindaraj and C. N. R. Rao, *J. Phys. Chem. C*, 2009, **113**, 11.
20 D. Du, P. Li and J. Ouyang, *ACS Appl. Mater. Interfaces*, 2015, **7**, 26952.
21 S. Park, J. An, J. R. Potts, A. Velamakanni, S. Murali and R. S. Ruoff, *Carbon*, 2011, **49**, 3019.
22 X. Fan, W. Peng, Y. Li, X. Li, S. Wang, G. Zhang and F. Zhang, *Adv. Mater.*, 2008, **20**, 4490.
23 N. A. Santos, S. S. Damasceno, P. H. M. D. Araujo, V. C. Marques, R. Rosenhaim, V. J. Fernandes, J. N. Queiroz, I. M. G. Santos, A. S. Maia and A. G. Souza, *Energy Fuels*, 2011, **25**, 4190.
24 S. A. S. Sunaga, T. Taniguchi, H. Miyazaki and T. Nabeshima, *Inorg. Chem.*, 2007, **46**, 2959.
25 P. Souza, J. A. G. Vazquez and J. R. Masaguer, *Transition Met. Chem.*, 1985, **10**, 410.
26 Y. Elerman, M. Kabak and A. Elmali, *Z. Naturforsch., B: J. Chem. Sci.*, 2002, **57**, 651.
27 X. Q. Ji, L. Cui, Y. H. Xu and J. Q. Liu, *Compos. Sci. Technol.*, 2015, **106**, 25.
28 N. An, F. H. Zhang, Z. A. Hu, Z. M. Li, L. Li, Y. Y. Yang, B. S. Guo and Z. Q. Lei, *RSC Adv.*, 2015, **5**, 23942.
29 W. S. Hummers and R. E. Offeman, *J. Am. Chem. Soc.*, 1958, **80**, 1339.

30 I. Correia, S. Roy, C. P. Matos, S. Borovic, N. Butenko, I. Cavaco, F. Marques, J. Lorenzo, A. Rodríguez, V. Moreno and J. C. Pessoa, *J. Inorg. Biochem.*, 2015, **147**, 134.
31 P. A. N. Reddy, M. Nethaji and A. R. Chakravarty, *Eur. J. Inorg. Chem.*, 2004, **7**, 1440.
32 K. Nagaraj, S. Sakthinathan and S. Arunachalam, *J. Iran. Chem. Soc.*, 2015, **12**, 267.
33 K. Nagaraj, S. Sakthinathan and S. Arunachalam, *J. Fluoresc.*, 2014, **24**, 589.
34 Z. Bo, X. Shuai, S. Mao, H. Yang, J. Qian, J. Chen, J. Yan and K. Cen, *Sci. Rep.*, 2014, **4**, 4684, DOI: 10.1038/srep04684.
35 H. Gou, J. He, Z. Mo, X. Wei, R. Hu and Y. Wang, *RSC Adv.*, 2015, **5**, 60638.
36 M. M. Seanu, I. Georgescu, L. E. Bibire and G. Carj, *Catal. Commun.*, 2014, **54**, 39.
37 K. M. Parida, M. Sahoo and S. Singha, *J. Mol. Catal. A: Chem.*, 2010, **329**, 7.
38 C. Y. Lin, A. Balamurugan, Y. H. Lai and K. C. Ho, *Talanta*, 2010, **82**, 1905.
39 G. Guidelli, F. Pergola and G. Raspi, *Anal. Chem.*, 1972, **44**, 745.
40 V. Mani, B. Dinesh, S. M. Chen and R. Saraswathi, *Biosens. Bioelectron.*, 2014, **53**, 420.
41 A. Afhami, F. S. Felehgari, T. Madrakian and H. Ghaedi, *Biosens. Bioelectron.*, 2014, **51**, 379.
42 S. J. Li, G. Y. Zhao, R. X. Zhang, Y. L. Hou, L. Liu and H. Pang, *Microchim. Acta*, 2013, **180**, 821.
43 V. Mani, A. P. Periasamy and S. M. Chen, *Electrochem. Commun.*, 2012, **17**, 75.
44 C. Yang, J. Xu and S. Hu, *J. Solid State Electrochem.*, 2007, **11**, 514.
45 G. R. Xu, G. Xu, M. L. Xu, Z. Zhang, Y. Tian, H. N. Choi and W. Y. Lee, *Bull. Korean Chem. Soc.*, 2012, **33**, 415.
46 S. Palanisamy, B. Thirumalraj and S. M. Chen, *J. Electroanal. Chem.*, 2016, **760**, 97.
47 K. Zhao, H. Song, S. Zhuang, L. Dai, P. He and Y. Fang, *Electrochem. Commun.*, 2007, **9**, 65.
48 A. R. Marlinda, A. Pandikumar, N. Yusoff, N. M. Huang and H. N. Lim, *Microchim. Acta*, 2015, **182**, 1113.
49 L. Zhang and E. M. Yi, *Bioprocess Biosyst. Eng.*, 2009, **32**, 485.
50 Y. Cui, C. Yang, W. Zeng, M. Oyama, W. Pu and J. Zhang, *Anal. Sci.*, 2007, **23**, 1421.
51 L. Zhang, F. Yuan, X. Zhang and L. Yang, *Chem. Cent. J.*, 2011, **5**, 75.
52 P. Miao, M. Shen, L. Ning, G. Chen and Y. Yin, *Anal. Bioanal. Chem.*, 2011, **399**, 2407.
53 R. Madhu, V. Veeramani and S. M. Chen, *Sci. Rep.*, 2041, **4**, 4679, DOI: 10.1038/srep04679.
54 X. Luo, A. J. Killard and M. R. Smyth, *Chem.–Eur. J.*, 2007, **13**, 2138.
55 W. Xue, L. Hui, W. Min, G. S. Li, Z. Yan, W. Q. Jiang, H. P. Gang and F. Y. Zhi, *Chin. J. Anal. Chem.*, 2013, **41**, 1232.